Brain, Behavior, & Immunity - Health 26 (2022) 100549

Contents lists available at ScienceDirect

Brain, Behavior, & Immunity - Health

journal homepage: www.editorialmanager.com/bbih/default.aspx

Estimation of blood-based biomarkers of glial activation related to neuroinflammation

Fumihiko Yasuno [a,b,*], Atsushi Watanabe [c], Yasuyuki Kimura [a,b], Yumeka Yamauchi [c], Aya Ogata [b,d], Hiroshi Ikenuma [b], Junichiro Abe [b], Hiroyuki Minami [a], Takashi Nihashi [a], Kastunori Yokoi [a], Saori Hattori [b], Nobuyoshi Shimoda [e], Kensaku Kasuga [f], Takeshi Ikeuchi [f], Akinori Takeda [a], Takashi Sakurai [a], Kengo Ito [a,b], Takashi Kato [a,b]

[a] National Hospital for Geriatric Medicine, National Center for Geriatrics and Gerontology, Obu, Japan
[b] Department of Clinical and Experimental Neuroimaging, Center for Development of Advanced Medicine for Dementia, National Center for Geriatrics and Gerontology, Obu, Japan
[c] Equipment Management Division, Center for Core Facility Administration, National Center for Geriatrics and Gerontology, Obu, Japan
[d] Department of Pharmacy, Faculty of Pharmacy, Gifu University of Medical Science, Kani, Japan
[e] Molecular Analysis Division, Center for Core Facility Administration, National Center for Geriatrics and Gerontology, Obu, Japan
[f] Department of Molecular Genetics, Brain Research Institute, Niigata University, Niigata, Japan

ARTICLE INFO

Keywords:
Neuroinflammation
Alzheimer's disease (AD)
Blood-based biomarkers
Positron emission tomography (PET)
Monocyte chemotactic protein 1 (MCP-1)
Soluble triggering receptor expressed on myeloid cells 2 (sTREM2)

ABSTRACT

Background: Neuroinflammation is a well-known feature of Alzheimer's disease (AD), and a blood-based test for estimating the levels of neuroinflammation would be expected. In this study, we examined and validated a model using blood-based biomarkers to predict the level of glial activation due to neuroinflammation, as estimated by ^{11}C-DPA-713 positron emission tomography (PET) imaging.

Methods: We included 15 patients with AD and 10 cognitively normal (CN) subjects. Stepwise backward deletion multiple regression analysis was used to determine the predictors of the TSPO-binding potential (BP_{ND}) estimated by PET imaging. The independent variables were age, sex, diagnosis, apolipoprotein E4 positivity, body mass index and the serum concentration of blood-based biomarkers, including monocyte chemotactic protein 1 (MCP-1), fractalkine, chitinase 3-like protein-1 (CHI3L1), soluble triggering receptor expressed on myeloid cells 2 (sTREM2), and clusterin.

Results: Sex, diagnosis, and serum concentrations of MCP1 and sTREM2 were determined as predictors of TSPO-BP_{ND} in the Braak1-3 area. The serum concentrations of MCP1 and sTREM2 correlated positively with TSPO-BP_{ND}. In a leave one out (LOO) cross-validation (CV) analysis, the model gave a LOO CV R^2 of 0.424, which indicated that this model can account for approximately 42.4% of the variance of brain TSPO-BP_{ND}.

Conclusions: We found that the model including serum MCP-1 and sTREM2 concentration and covariates of sex and diagnosis was the best for predicting brain TSPO-BP_{ND}. The detection of neuroinflammation in AD patients by blood-based biomarkers should be a sensitive and useful tool for making an early diagnosis and monitoring disease progression and treatment effectiveness.

1. Introduction

Neuroinflammation is one of the critical aspects of Alzheimer's disease (AD) that contribute to its pathogenesis and pathological signs (Zhang et al., 2013). Pathological amyloid β (Aβ) and neurofibrillary tangle (NFT) accumulation is regarded to be the cause of neuroinflammatory responses in AD, stimulating resident glial activation (Serrano-Pozo et al., 2011). The practical method for evaluating cerebral neuroinflammatory levels in-vivo is positron emission tomography (PET) imaging with radioligands binding to 18 kDa translocator protein (TSPO) increased by the glial activation due to neuroinflammation, including ^{11}C-PBR28 (Fujita et al., 2008), ^{11}C-DAA1106

* Corresponding author. National Hospital for Geriatric Medicine, National Center for Geriatrics and Gerontology, 7-430 Morioka-cho, Obu, Aichi, 474-8511, Japan.
E-mail address: yasunof@ncgg.go.jp (F. Yasuno).

https://doi.org/10.1016/j.bbih.2022.100549
Received 19 July 2022; Received in revised form 8 October 2022; Accepted 30 October 2022
Available online 5 November 2022

(Yasuno et al., 2008, 2012), and ^{11}C-DPA-713 (Boutin et al., 2007; Yasuno et al., 2022). However, PET scanning is expensive and limited to specialized centers, and it is not a candidate for screening. An inexpensive, noninvasive screening approach that correctly evaluates the level of neuroinflammation would satisfy a critical need in geriatric patients.

Cerebrospinal fluid (CSF) biomarke is one of candidates for the evaluation of glial activation due to neuroinflammation. In the adult the interface between the CSF and the brain is lined by the cerebrospinal fluid-brain barrier (CSFBB) formed by ependymal cells, which limit the exchange of different sized molecules between cerebrospinal fluid and the brain parenchyma. However, the limitation of CSFBB is less restrictive than that of blood-brain barrier (BBB) and CSF biomarker has the advantage for the evaluation of the state of the brain when compared to blood biomarker in terms of accuracy. The clinical data of AD patients have shown an increase of CSF biomarkers of glial activation such as monocyte chemotactic protein 1 (MCP-1) (Corrêa et al., 2011), chitinase 3-like protein-1 (CHI3L1) (Antonell et al., 2014; Craig-Schapiro et al., 2010) and soluble triggering receptors expressed on myeloid cells 2 (sTREM2) (Heslegrave et al., 2016) compared to the healthy controls. These studies showed possible utility of CSF biomarkers of glial activation due to neuroinflammation. However, the availability of CSF is also restricted in standard clinical situations because of the invasiveness of lumbar punctures for its collection. As a more available biological source, recent studies are in search of the blood biomarkers of neuroinflammation (Angiulli et al., 2021).

Although the central nervous system (CNS) is separated from the peripheral immune system by the blood-brain barrier (BBB) (Daneman and Prat, 2015), proinflammatory mediators, such as cytokines, chemokines, and nitric oxide, can modify the BBB permeability (Wong et al., 2004). Glial activation results in the release of soluble inflammatory mediators that cross the BBB and move to the periphery via the bloodstream, thereby leading to the proliferation of peripheral immune cells (Fiala et al., 1998). The CNS is also reactive to changes in the peripheral immune system. Proinflammatory cytokines emitted by peripheral immune cells are transported to the BBB by the bloodstream, crossing the brain parenchyma and acting on glial cells (Krstic et al., 2012). This evidence of the relationship between the central and peripheral immune systems suggests the utility of the blood compartment as an origin of potential biomarkers of neuroinflammation (Angiulli et al., 2021).

In this study, we aimed to examine and validate a model using blood-based biomarkers that can predict the level of glial activation due to neuroinflammation, as estimated by ^{11}C-DPA-713 PET imaging of TSPO. ^{11}C-DPA-713 was used in this study because we confirmed in our previous study that it possessed the properties suitable for TSPO quantification with PET imaging in our research environment, and showed that non-displaceable binding potential can be estimated stably with this ligand by using the Braak 6 area as the reference region (Yasuno et al., 2022).

Stepwise backward deletion multiple regression analysis was used to determine the predictors of TSPO-binding potential (BP_{ND}) estimated by ^{11}C-DPA-713 PET imaging. The dependent variable was TSPO-BP_{ND}, and the independent variables were age, sex, diagnosis, apolipoprotein (APO) E4 positivity, body mass index (BMI), which have a potential impact on pathophysiology of AD (Fernández-Calle et al., 2022; Lloret et al., 2019; Podcasy and Epperson, 2016) and the serum concentrations of the blood-based biomarker candidates, which are known to be related to glial activation and are shown to affect the pathophysiology of AD, including MCP-1 (Johnstone et al., 1999; Meda et al., 1996; Sanchez-Sanchez et al., 2022), fractalkine (Chidambaram et al., 2020; Zujovic et al., 2000), CHI3L1 (Bonneh-Barkay et al., 2010; Connolly et al., 2022), sTREM2 (Shi and Holtzman, 2018; Zhong et al., 2019), and clusterin (Spatharas et al., 2022; Xie et al., 2005).

2. Materials and methods

2.1. Participants and ethics

This study included 15 patients diagnosed with AD and 10 cognitively normal (CN) subjects. The inclusion criteria were as follows: for AD, Mini-Mental State Examination (MMSE) scores less than 24 and meeting the National Institute on Aging and Alzheimer's Association (NIA-AA) clinical criteria for probable AD (McKhann et al., 2011). For CN, MMSE score 24–30, Clinical Dementia Rating (CDR) score = 0, and non-demented status. The participants in this study were required to be between 65 and 85 years old (inclusive). None of the subjects was on treatment for any substantial medical, neurological, or psychiatric disease or had any history of a major psychiatric disorder, alcohol dependence, or substance dependence. No individuals showed clinically significant focal brain lesions on magnetic resonance imaging (MRI). All of the patients with AD and 3 of the 10 CN subjects were shown to be amyloid positive by analyzing cerebrospinal fluid (CSF) Aβ42/40 ratio values at the Brain Research Institute of Niigata University, with a cut-off value of <0.072 determined based on 177 CSF samples from the Japanese Alzheimer's Disease Neuroimaging Initiative (Delaby et al., 2021). BMI was calculated by dividing the weight in kg by the square of the height in m.

All selected subjects had stored blood samples and corresponding ^{11}C-DPA-713 PET imaging data. All participants were classified as having high-affinity binders based on the rs6971 polymorphism within the *TSPO* gene (Owen et al., 2011). APOE4 genotypes were determined from deoxyribonucleic acid (DNA) using polymerase chain reaction amplification (Hixson and Vernier, 1990). The quantification of the TSPO was done using dynamic ^{11}C-DPA-713 PET imaging data with arterial blood sampling (Yasuno et al., 2022). We measured the serum concentrations of MCP-1, fractalkine, CHI3L1, sTREM2, and clusterin as candidates for blood-based biomarkers that are known to be related to glial activation.

This study was approved by the institutional review board of the National Center for Geriatrics and Gerontology, and all participants provided written informed consent.

2.2. Blood collection and serum biomarker assay

Serum was isolated from whole blood by centrifugation, aliquoted, and stored at −80 °C in the National Center for Geriatrics and Gerontology (NCGG) biobank. Serum levels of MCP-1, fractalkine, CHI3L1, TREM2, and clusterin were measured using enzyme-linked immunosorbent assay (ELISA) kits. The MCP-1, fractalkine, CHI3L1, and clusterin kits were purchased from R&D Systems, Inc. (Minneapolis, MN, USA), and the sTREM2 kit was purchased from AB clonal, Inc. (Woburn, MA, USA). The ELISA was performed according to the manufacturer's protocol described in the kit. The optical density of each plate was determined using a Spectra Max Paradigm microplate reader (Molecular Devices LLC. San Jose, CA, USA).

2.3. PET image acquisition and analysis

^{11}C-DPA-713 is a PET radiotracer developed for imaging the expression of TSPO in glial cells, a marker of neuroinflammatory burden. The details of the PET image acquisition and analysis methods have been described in our previous study (Yasuno et al., 2022).

All PET scans were obtained using a PET CT camera (Biograph True V; Siemens Healthcare, Erlangen, Germany). All participants underwent 3D PET imaging for 0–60 min after bolus-intravenous injection of 411.2 ± 38.0 MBq of ^{11}C-DPA-713 (range, 251–452 MBq). The mean and SD of the administered amount of ^{11}C-DPA-713 were 6.1 ± 2.0 nmol (range, 2.9–10.5 nmol). Time bins were 6 × 10, 3 × 20, 2 × 60, 2 × 180, and 10 × 300 s for the 60 min. Arterial samples were taken manually, and their radioactivity concentration was measured every 10 s initially after the

injection and reduced in frequency every 15 min until the end of the scan. Arterial blood samples for metabolite analysis were drawn manually at 5, 15, 30, 45, and 60 min. PET images were corrected for scattering, attenuation, and time-of-flight and reconstructed using the ordered subset expectation maximization method. The final reconstructed images consisted of 109 planes of 168 × 168 voxels of 2.04 × 2.04 × 2.03 mm^3. Dynamic PET images were motion-corrected and registered into the standard Montreal Neurological Institute (MNI) space using the P-mod View tool and the Registration and Fusion tool (PMOD Technologies). Motion correction was performed frame-by-frame through rigid body registration of adjacent frames, and motion-corrected PET images were scaled to a standardized uptake value (SUV) and spatially normalized in the MNI stereotactic space with parameters obtained from the transformation of individual 3D-T1 MR images, which were co-registered to PET images into the MNI space using affine registration followed by nonlinear warping. A region of interest template from the Automated Anatomical Labeling (AAL) atlas (Tzourio-Mazoyer et al., 2002) was applied to the spatially normalized PET images to obtain a regional SUV.

The regional SUV was quantified in ROIs that anatomically approximated the pathological stages of tangle deposition delineated by Braak and Braak (1991). Time-activity curves (TACs) were calculated from the cerebellum, and three composite ROIs that corresponded to the anatomical definitions of Braak stages 1 to 3 (the transentorhinal and entorhinal region and the neocortex of the fusiform and lingual gyri), stage 4 (the neocortical limbic areas and temporal region), stage 5 (the neocortical region extending in a fan-like projection to the frontal, superolateral, and occipital directions), and stage 6 (the areas including the secondary and primary neocortical regions of the occipital lobe, extending into the striate area) (Braak et al., 2006) (Table 1).

Regional time-activity data were analyzed using one-tissue compartment models with a variable vascular fraction using the metabolite-corrected plasma input function. Two rate constants (K_1 and k_2) were derived from this model and fitted to determine the total distribution volume (V_T) = K_1/k_2. Binding potential (BP_{ND}) was calculated using the formula (V_T^{tissue} - $V_T{}^{ref}$)/$V_T{}^{ref}$, where V_T^{tissue} is the V_T of the target tissue and $V_T{}^{ref}$ is the V_T of the reference tissue. We used the Braak 6 area as a reference tissue region for TSPO quantification with ^{11}C-DPA-713-PET imaging, as the Braak 6 area was shown to be a non-target of ^{11}C-DPA-713 in mild to moderate AD in a previous study (Yasuno et al., 2022).

2.4. Statistics

Statistical analysis was performed using log10 transformation of the serum concentration of blood-based biomarkers to better approximate normality. Stepwise backward deletion multiple regression analysis was used to determine the predictors of brain PET-TSPO-BP_{ND}. The dependent variable was PET-TSPO-BP_{ND}, and the independent variables were age, sex (coded with male as 0 and female as 1), diagnosis (coded with CN as 0 and AD as 1), APOE4 positivity (coded with negative as 0 and positive as 1), BMI, and serum concentration of the blood-based biomarkers related to glial activation.

After identifying the blood-based biomarkers and covariates in the best model for predicting brain PET-TSPO-BP_{ND} in the above analysis, a leave-one-out (LOO) cross-validation (CV) analysis was performed by fitting the identified multiple linear regression model to the data, leaving out one subject at a time, and using the model to predict brain TSPO-BP_{ND} in that subject based on the fitted model (Kiddle et al., 2012). LOO CV R^2 was calculated as the square of the Pearson's correlation coefficient between the predicted and the observed brain PET-TSPO-BP_{ND}.

Statistical tests were two-tailed, and significance was defined as $p < 0.05/n$ using the Bonferroni correction (where n refers to the number of multiple comparisons).

Table 1
Region of interests (ROIs) information.

Region of interests (ROIs)	Volume (cm^3)	Corresponding region in Automated Anatomical Labeling (AAL) atlas
Braak stages 1 to 3	109.43	Hippocampal and parahippocampal region, amygdala, lingual area, fusiform area
Braak stage 4	299.14	Insular, anterior, middle and posterior cingulum, temporal area
Braak stage 5	637.76	Rolandic and operculum area, superior motor area, superior, middle, and inferior frontal areas, rectus, occipital area, supramarginal area, angular area, precuneus area, Heschl area, parietal area
Braak stage 6	191.01	Precentral area, calcarine area, cuneus area, postcentral area, paracentral lobule

3. Results

3.1. Demographics and serum concentration of blood-based biomarkers in CN and AD groups

The basic demographics of the study population are summarized in Table 2. A total of 10 CN and 15 AD participants were evaluated. We found higher TSPO-BP_{ND} in the Braak1-3 areas in the AD group than in the CN group (Table 2).

In the comparison of the serum concentrations of the candidate blood-based biomarkers of glial activation between the CN and AD groups, we found no significant difference between the CN and AD groups, with p-values less than 0.01 using Bonferroni correction (Table 3).

3.2. Stepwise backward deletion multiple regression analysis predicting the brain TSPO-BP_{ND}

Stepwise backward deletion multiple linear regression analysis was performed to determine which factors were the best predictors of TSPO-BP_{ND} in Braak1-3 areas; a significant increase was shown in the AD group. The dependent variable was TSPO-BP_{ND} in Braak1-3 areas. The independent variables were age, sex, diagnosis (CN vs. AD), APOE4 positivity, BMI, and log10 conversion of serum concentrations of CHI3L1 (ng/mL), MCP-1 (pg/mL), clusterin (μg/mL), fractalkine (pg/mL), and sTREM2 (pg/mL). Age, APOE4 positivity, and serum concentrations of CHI3L1, clusterin, and fractalkine were removed, while sex, diagnosis, and serum concentrations of MCP1 and sTREM2 were included in the final model as predictors of TSPO-BP_{ND} in Braak1-3 areas [R^2 = 0.396, effect size = $R^2/(1-R^2)$ = 0.656, total sample size = 25, number of predictors = 4] (Table 4). When we evaluated the statistical power with α = 0.05 with G* Power software (© 2021 Heinrich-Heine-Universität Düsseldorf, Germany), we found the adequate value of 0.84 (>0.80).

The analysis revealed that, in all individuals, the log10 conversion of the serum concentrations of MCP1 and sTREM2 correlated positively with TSPO-BP_{ND} (β = 0.51 and 0.60 for MCP1 and TREM2, respectively). Fig. 1 shows a visual representation of the association between the log10 conversion of serum concentrations of MCP1/sTREM2 and TSPO-BP_{ND} in Braak1-3 areas in all individuals after adjusting for other independent variables within the model.

TSPO-BP_{ND} in the Braak 1–3 area and the serum concentration of MCP-1 were adjusted for sex, diagnosis, and serum sTREM2 concentration) (left), and TSPO-BP_{ND} and the serum concentration of sTREM2 were adjusted for sex, diagnosis, and serum MCP-1 concentration) (right). The line shows the linear fit of TSPO-BP_{ND} in the Braak 1–3 area with MCP-1 (r = 0.51, p = 0.007) (left) and sTREM2 concentrations (r = 0.60, p = 0.002) (right)

In the validation analysis, the multiple linear regression with the log10 conversion of the serum concentrations of MCP1 and TREM2 and covariates of sex and diagnosis gave a LOO CV R^2 of 0.424. This model accounted for approximately 42.4% of the variance in brain TSPO-BP_{ND}

Table 2
Descriptive Characteristics of the CN and AD participants [mean ± SD (min-max)].

Characteristic/Test	All	CN	AD	t or χ^2	P
No.	25	10	15		
Sex, M/F	11/14	4/6	7/8	0.11	0.74
Age, yr	78.4 ± 4.4 (69–85)	78.9 ± 5.2 (69–85)	78.1 ± 3.9 (70–84)	0.42	0.68
Education, yr	12.4 ± 2.4 (9–16)	13.0 ± 2.3 (9–16)	11.9 ± 2.5 (9–16)	1.09	0.29
MMSE	22.9 ± 3.6 (15–29)	26.2 ± 2.2 (24–29)	20.7 ± 2.4 (15–23)	5.76	<0.001*
ApoE4 (+)/(−)	13/12	4/6	9/6	0.96	0.33
BMI	22.4 ± 3.9 (14.2–30.1)	23.0 ± 5.6 (14.2–30.1)	22.0 ± 2.4 (18.8–26.4)	0.57	0.58
DPA-713 TSPO-PET results					
Braak 1–3-TSPO-BP_{ND} (medial temporal area)	0.14 ± 0.07 (0.04–0.28)	0.10 ± 0.05 (0.04–0.16)	0.18 ± 0.07 (0.07–0.28)	−3.23	0.004*
Braak 4-TSPO-BP_{ND} (limbic area)	0.09 ± 0.07 (−0.01–0.24)	0.07 ± 0.07 (0.00–0.24)	0.10 ± 0.07 (−0.01–0.22)	−1.12	0.27
Braak 5-TSPO-BP_{ND} (neocortical area)	0.00 ± 0.04 (−0.06–0.10)	−0.01 ± 0.05 (−0.06–0.10)	0.00 ± 0.04 (−0.05–0.08)	−0.54	0.60

*P<0.05.
Abbreviations: CN, cognitively normal; AD, Alzheimer's disease; MMSE, Mini-mental state examination; BMI, body mass index; TSPO, translocator protein: BPND, binding potential.

Table 3
Serum and plasma concentrations of the candidate blood-based biomarkers of glial activation related to neuroinflammation [mean ± SD (min-max)].

Candidate blood-based biomarker	All (n = 25)	CN (n = 10)	AD (n = 15)	Mann-Whitney U	Z	P
CHI3L1 (ng/mL)	90.7 ± 62.0 (1.5–255.1)	89.7 ± 66.2 (29.9–213.7)	97.8 ± 62.8 (32.9–255.1)	65.0	−0.56	0.579
MCP-1(pg/mL)	137.2 ± 42.0 (0.8–205.7)	131.6 ± 32.0 (76.5–190.7)	148.7 ± 34.6 (84.2–205.7)	52.0	−1.28	0.202
Clusterin (μg/mL)	312.4 ± 150.6 (1.31–825.4)	322.4 ± 104.3 (141.7–478.6)	327.1 ± 171.1 (130.0–825.4)	71.0	−0.22	0.824
Fractalkine (pg/mL)	0.50 ± 0.16 (0.29–0.82)	0.39 ± 0.08 (0.29–0.51)	0.56 ± 0.17 (0.32–0.82)	29.5	−2.52	0.012
sTREM2 (pg/mL)	6.01 ± 6.18 (0.01–30.0)	8.31 ± 8.49 (0.04–30.0)	4.35 ± 4.06 (0.01–12.3)	50.0	−1.39	0.166

*P<0.01(0.05/5).
Abbreviations: CN, cognitively normal; AD, Alzheimer's disease; CHI3L1, chitinase 3-like protein-1; MCP-1, monocyte chemotactic protein 1; sTREM2, soluble triggering receptor expressed on myeloid cells 2.

(Fig. 2).

The line shows the linear fit of the real and predicted values of TSPO-BP_{ND} in the Braak 1–3 area (r = 0.65, p<0.001).

4. Discussion

The main focus of this study was to find a model with blood-based biomarkers that can predict the level of glial activation due to neuroinflammation, as shown by PET-TSPO-BP_{ND} in CN and AD participants. We found that the model including serum MCP-1 and sTREM2 with covariates of sex and diagnosis could predict brain TSPO-BP_{ND} in the Braak 1–3 area, which showed a significant increase in the AD group.

Neuroinflammation is a core pathological aspect of AD, and inflammatory responses are caused by the aggregation of Aβ and NFT, inducing resident glial activation (Serrano-Pozo et al., 2011). Upon activation, glial cells show increased levels of TSPO (Banati et al., 2004), which is an 18-kDa protein shown mainly on the outer mitochondrial membrane (Papadopoulos et al., 2006), and TSPO is regarded as a landmark of the inflammatory response in disease states. In humans, the burden of neuroinflammation has been evaluated using PET with TSPO radiotracers. However, PET is relatively expensive, and its availability is limited. Furthermore, PET results in cumulative radiation exposure of the subjects. As a more available biological source, blood is useful because its collection is less invasive, inexpensive, reproducible, and easy to conduct on large populations. Glial activation induces the release of soluble inflammatory mediators that cross the BBB (Fiala et al., 1998), and they are expected to be used as blood-based biomarkers for predicting the level of glial activation due to neuroinflammation.

In the previous studies, increased peripheral levels of proinflammatory cytokines including IL-6, IL-1β and TNF-α and anti-inflammatory cytokine of TGF-β have been reported in AD patients compared to healthy controls (Alvarez et al., 2007; Fillit et al., 1991; Forlenza et al., 2009; Malaguarnera et al., 2006; Wu et al., 2015). As to the peripheral chemokine, the clinical data of AD patients have shown an increase of peripheral MCP-1 (Galimberti et al., 2006), IL8 (Alsadany et al., 2013), CHI3L1 (Choi et al., 2011) compared to the healthy controls. In the prospective cohort study, the significant association was shown between increased serum sTREM2 levels and the risk of developing AD in the general elderly Japanese population (Ohara et al., 2019). The serum neuroinflammation biomarker signatures were shown to improve the accuracy of classification for AD pathology in older adults (Popp et al., 2017). These studies indicated the relationship between underlying neurodegenerative processes in AD and blood-based biomarkers of neuroinflammation. However, there are currently no blood tests for reliably and directly estimating the level of cerebral neuroinflammation determined by practical method of TSPO-PET imaging. Our study is the first to reveal the model with blood-based neuroinflamamtion biomarker whch could predict brain TSPO-BP_{ND}.

In our study of blood-based biomarkers of glial activation, stepwise backward deletion multiple regression models showed that the model including serum MCP-1 and sTREM2 with covariates of sex and diagnosis was the best at predicting brain TSPO-BP_{ND} in the Braak 1–3 area, of which a significant increase was shown in the AD group. This model could explain >40% of the variance in TSPO-BP_{ND}. This result indicated that serum concentrations of MCP-1 and sTREM2 can predict the levels of glial activation, as shown by PET-TSPO imaging, indicating the utility of serum MCP-1 and sTREM2 as blood-based biomarkers for neuroinflammation.

Covariates of sex (coded with male as 0 and female as 1) showed positive β values in the final model. This indicated that being female promotes an increase in TSPO-BP_{ND} in the Braak 1–3 area. Over the life course, females are shown to be more likely than men to develop AD (Gao et al., 1998). Sex may influence the incidence of AD via genetic (Dumitrescu et al., 2019; Nazarian et al., 2019), hormonal (Viña and Lloret, 2010), and lifestyle mechanisms (Barha and Liu-Ambrose, 2018; Yusufov et al., 2017), and these sex differences may create a neuronal vulnerability of females against the pathology of AD and promote the inflammatory changes shown as an increase in TSPO-BP_{ND}.

Although the serum concentrations of MCP-1 and sTREM2 had opposite trends in AD (increasing and decreasing, respectively), after adjusting for the effects of the other predictors, a partial residual plot of TSPO-BP_{ND} in the Braak 1–3 area against them showed that both of them

Table 4
Results of a stepwise backward deletion multiple linear regression analysis predicting Braak 1–3 -TSPO-BPND.

Step	t	β	P	F	df	P	Adjusted R2
Model 1				2.57	10, 14	0.05	0.396
Age	0.19	0.04	0.85				
Sex	1.68	0.37	0.11				
Diagnosis (CN vs AD)	3.02	0.64	0.009				
ApoE4 positivity	0.11	0.02	0.91				
BMI	0.81	0.14	0.43				
CHI3L1 (ng/mL)	−0.43	−0.09	0.68				
MCP-1 (pg/mL)	2.27	0.53	0.04				
Clusterin (μg/mL)	0.10	0.02	0.92				
Fractalkine (pg/mL)	−0.14	−0.04	0.89				
sTREM2 (pg/mL)	2.83	0.62	0.01				
Model 2				3.06	9, 15	0.03	0.436
Age	0.18	0.03	0.86				
Sex	2.07	0.36	0.06				
Diagnosis (CN vs AD)	3.12	0.64	0.007				
ApoE4 positivity	0.10	0.02	0.92				
BMI	0.83	0.14	0.42				
CHI3L1 (ng/mL)	−0.43	−0.09	0.67				
MCP-1 (pg/mL)	2.34	0.53	0.03				
Fractalkine (pg/mL)	−0.12	−0.03	0.90				
sTREM2 (pg/mL)	3.12	0.62	0.007				
Model 3				3.67	8, 16	0.01	0.470
Age	0.18	0.03	0.86				
Sex	2.14	0.36	0.05				
Diagnosis (CN vs AD)	3.3	0.64	0.004				
BMI	0.85	0.14	0.41				
CHI3L1 (ng/mL)	−0.45	−0.08	0.66				
MCP-1 (pg/mL)	2.44	0.53	0.03				
Fractalkine (pg/mL)	−0.12	−0.03	0.9				
sTREM2 (pg/mL)	3.24	0.62	0.005				
Model 4				4.44	7, 17	0.006	0.501
Age	0.23	0.04	0.82				
Sex	2.25	0.35	0.04				
Diagnosis (CN vs AD)	4	0.62	0.001				
BMI	0.87	0.13	0.39				
CHI3L1 (ng/mL)	−0.45	−0.07	0.66				
MCP-1 (pg/mL)	2.85	0.52	0.01				
sTREM2 (pg/mL)	3.41	0.63	0.003				
Model 5				5.46	6,18	0.002	0.527
Sex	2.4	0.36	0.03				
Diagnosis (CN vs AD)	4.12	0.62	0.001				
BMI	0.87	0.13	0.40				
CHI3L1 (ng/mL)	−0.41	−0.06	0.69				
MCP-1 (pg/mL)	3.02	0.52	0.007				
sTREM2 (pg/mL)	3.53	0.63	0.002				
Model 6				6.82	5, 19	0.001	0.548
Sex	2.43	0.35	0.03				
Diagnosis (CN vs AD)	4.2	0.61	<0.001				
BMI	0.85	0.12	0.41				
MCP-1 (pg/mL)	3.06	0.52	0.006				
sTREM2 (pg/mL)	3.64	0.61	0.002				
Model 7				8.47	4, 20	<0.001	0.554
Sex	2.30	0.32	0.03				
Diagnosis (CN vs AD)	4.15	0.59	<0.001				
MCP-1 (pg/mL)	3.03	0.51	0.007				
sTREM2 (pg/mL)	3.60	0.60	0.002				

For serum concentration of blood-based biomarkers the log10 conversion were performed.
R2 = Multiple regression value squared.
Abbreviations: TSPO, translocator protein: BPND, binding potential; CN, Cognitively normal; AD, Alzheimer's disease; BMI, body mass index; CHI3L1, chitinase 3-like protein-1; MCP-1, monocyte chemotactic protein 1; sTREM2, soluble triggering receptor expressed on myeloid cells 2.

were positively correlated with TSPO-BP_{ND}. Previous clinical data have revealed an increase in MCP-1 levels in the periphery of patients with AD (Kim et al., 2011). MCP-1 is the chemokine that recruits and gathers immune cells at the site of Aβ aggregation. The increase in MCP-1 promoted by Aβ aggregation was revealed in glial cells and monocytes (Johnstone et al., 1999; Meda et al., 1996); it is conceivable that Aβ-induced MCP-1 production is associated with a trial of glial cells to remove Aβ pathology by the recruitment of phagocytic cells (Kiyota et al., 2013; Peterson et al., 1997), although its overexpression may cause harmful inflammatory effects on the brain (Sokolova et al., 2009).

TREM2 is a membrane-bound protein found in Aβ-related microglia and peripherally recruited monocytes/macrophages in the AD brain (Fahrenhold et al., 2018; Frank et al., 2008; Jay et al., 2015). Genome-wide association studies identified TREM2 as one of the strongest genetic risk factors for AD (Karch and Goate, 2015). After combining with oligomeric Aβ (Lessard et al., 2018), TREM2 facilitates

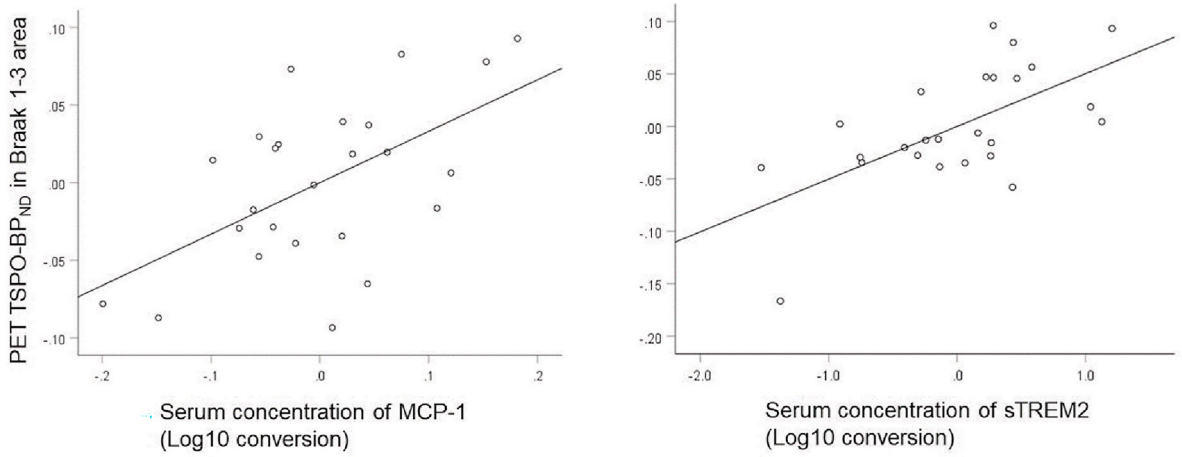

Fig. 1. Partial residual plot of TSPO-BP$_{ND}$ in the Braak 1–3 area against the serum concentrations of MCP-1 (left) and sTREM2 (right) (Log10 conversion values) while adjusting for the effects of the other predictors.

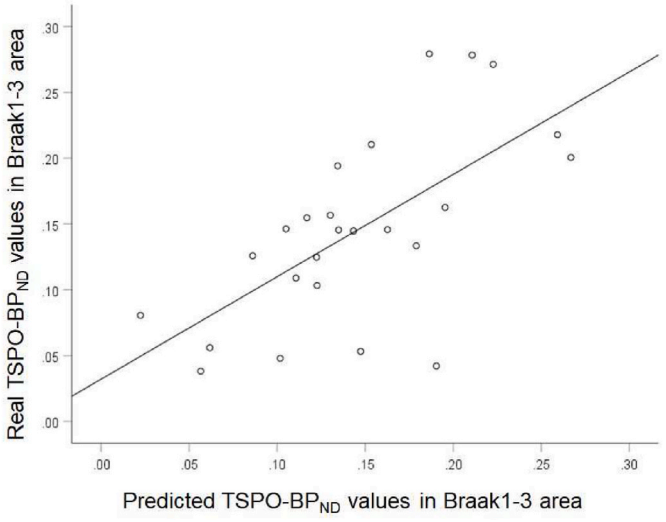

Fig. 2. Scatter plot of individual real and predicted TSPO-BPND values in the Braak 1–3 area with a leave one out (LOO) cross-validation (CV) analysis.

the accumulation of myeloid cells around Aβ aggregates (Jay et al., 2015; Ulrich et al., 2014) and the uptake and elimination of Aβ (Claes et al., 2019; Zhao et al., 2018). Under the consideration of these premises, it is conceivable that TREM2 plays a protective role in the early stages of AD. Furthermore, TREM2 is degraded by proteolysis and released in its soluble form (sTREM2) (Wunderlich et al., 2013). sTREM2 is supposed to have many functional features like those of full-length TREM2, such as binding with oligomeric Aβ and the recruitment of microglia, which is related to the reduction in Aβ aggregation (Zhong et al., 2019). Hence, the positive correlation between serum MCP-1 and sTREM2 and TSPO-BP$_{ND}$ may reflect the neuroinflammatory responses of glial cells induced by MCP-1 and sTREM2 to eliminate Aβ deposits.

It is unclear whether changes in serum levels of MCP-1 and sTREM2 are a cause or consequence of glial activation, as shown by TSPO-BP$_{ND}$. As previously mentioned, glial activation induces the release of soluble inflammatory mediators that cross the BBB (Fiala et al., 1998). Therefore, peripheral MCP-1 and sTREM2 are thought to be based on their leakage from the CNS, and they could be regarded as a reflection of glial activation in the CNS. Simultaneously, the CNS reacts to the activation of the peripheral immune system, and proinflammatory cytokines emitted by peripheral immune cells move towards the BBB (Krstic et al., 2012). In that sense, the peripheral immune cells activated by serum MCP-1 and sTREM2 and their emitted proinflammatory cytokines may cross the BBB and affect glial activation in the CNS. It was assumed that there was a mutual relationship between serum MCP-1 and sTREM2 and cerebral glial activation due to neuroinflammation.

A limitation of this study was the relatively restricted number of subjects, and it was inappropriate to divide the participants into training and test groups to assess the predictive accuracy of the regression model. In this study, we used a leave-one-out cross-validation approach to maximize the use of the available subjects (Kiddle et al., 2012). Given the restricted number of participants on which the model is dependent, it is desirable to confirm the capability of these biomarkers to estimate the level of brain neuroinflammation in an independent cohort. Further, 3 of the 10 CN subjects were shown to be amyloid positive by analyzing CSF Aβ42/40 ratio values. However, when we excluded these three amyloid-positive CN subjects in stepwise backward deletion multiple linear regression analysis, we found that the final model including serum MCP-1 and sTREM2 with covariates of sex and diagnosis could predict brain TSPO-BP$_{ND}$ in the Braak 1–3 area (t, β, and p-value are 2.39, 0.35, 0.03 for sex, 3.83, 0.61, 0.001 for diagnosis, 2.20, 0.41, 0.04 for MCP-1, and 3.10, 0.55, 0.007 for sTREM2, respectively)($F = 7.82$, $df = 4,17$, $p = 0.001$, adjusted $R^2 = 0.57$).

In conclusion, we found that the blood-based model including serum MCP-1 and sTREM2 and covariates of sex and diagnosis was the best at predicting brain TSPO-BP$_{ND}$ in the Braak 1–3 area, of which a significant increase was shown in the AD group. The detection of CNS neuroinflammation in patients with AD using blood-based biomarkers should be a sensitive and useful tool for early diagnosis and monitoring disease progression and treatment effectiveness.

Funding

This study received funding from the Japan Society for the Promotion of Science (KAKENHI Grant Number:24590908), National Center for Geriatrics and Gerontology [Research Funding for Longevity Sciences (23–26, 29-29)] to FY, and the Japan Agency for Medical Research and Development (AMED Grant Number: JP22dk0207059 and JPdm0207073) to TI.

Declaration of competing interest

The authors declare no potential conflicts of interest.

Data availability

Data will be made available on request.

Acknowledgments

We wish to thank Yoko Arai for patient care and Hiroshi Morisihita and other radiology technicians for their support with the PET scans.

References

Alsadany, M.A., Shehata, H.H., Mohamad, M.I., Mahfouz, R.G., 2013. Histone deacetylases enzyme, copper, and IL-8 levels in patients with Alzheimer's disease. Am J Alzheimers Dis Other Demen 28, 54–61.

Alvarez, A., Cacabelos, R., Sanpedro, C., García-Fantini, M., Aleixandre, M., 2007. Serum TNF-alpha levels are increased and correlate negatively with free IGF-I in Alzheimer disease. Neurobiol. Aging 28, 533–536.

Angiulli, F., Conti, E., Zoia, C.P., Da Re, F., Appollonio, I., Ferrarese, C., Tremolizzo, L., 2021. Blood-based biomarkers of neuroinflammation in Alzheimer's disease: a central role for periphery? Diagnostics 11.

Antonell, A., Mansilla, A., Rami, L., Lladó, A., Iranzo, A., Olives, J., Balasa, M., Sánchez-Valle, R., Molinuevo, J.L., 2014. Cerebrospinal fluid level of YKL-40 protein in preclinical and prodromal Alzheimer's disease. J Alzheimers Dis 42, 901–908.

Banati, R.B., Egensperger, R., Maassen, A., Hager, G., Kreutzberg, G.W., Graeber, M.B., 2004. Mitochondria in activated microglia in vitro. J. Neurocytol. 33, 535–541.

Barha, C.K., Liu-Ambrose, T., 2018. Exercise and the aging brain: considerations for sex differences. Brain Plast. 4, 53–63.

Bonneh-Barkay, D., Wang, G., Starkey, A., Hamilton, R.L., Wiley, C.A., 2010. In vivo CHI3L1 (YKL-40) expression in astrocytes in acute and chronic neurological diseases. J. Neuroinflammation 7, 34.

Boutin, H., Chauveau, F., Thominiaux, C., Grégoire, M.C., James, M.L., Trebossen, R., Hantraye, P., Dollé, F., Tavitian, B., Kassiou, M., 2007. 11C-DPA-713: a novel peripheral benzodiazepine receptor PET ligand for in vivo imaging of neuroinflammation. J. Nucl. Med. 48, 573–581.

Braak, H., Alafuzoff, I., Arzberger, T., Kretzschmar, H., Del Tredici, K., 2006. Staging of Alzheimer disease-associated neurofibrillary pathology using paraffin sections and immunocytochemistry. Acta Neuropathol. 112, 389–404.

Braak, H., Braak, E., 1991. Neuropathological stageing of Alzheimer-related changes. Acta Neuropathol. 82, 239–259.

Chidambaram, H., Das, R., Chinnathambi, S., 2020. Interaction of Tau with the chemokine receptor, CX3CR1 and its effect on microglial activation, migration and proliferation. Cell Biosci. 10, 109.

Choi, J., Lee, H.W., Suk, K., 2011. Plasma level of chitinase 3-like 1 protein increases in patients with early Alzheimer's disease. J. Neurol. 258, 2181–2185.

Claes, C., Van Den Daele, J., Boon, R., Schouteden, S., Colombo, A., Monasor, L.S., Fiers, M., Ordovás, L., Nami, F., Bohrmann, B., Tahirovic, S., De Strooper, B., Verfaillie, C.M., 2019. Human stem cell-derived monocytes and microglia-like cells reveal impaired amyloid plaque clearance upon heterozygous or homozygous loss of TREM2. Alzheimers Dement 15, 453–464.

Connolly, K., Lehoux, M., O'Rourke, R., Assetta, B., Erdemir, G.A., Elias, J.A., Lee, C.G., Huang, Y.A., 2022. Potential role of chitinase-3-like protein 1 (CHI3L1/YKL-40) in neurodegeneration and Alzheimer's disease. Alzheimers Dement. https://doi.org/10.1002/alz.12612. In press.

Corrêa, J.D., Starling, D., Teixeira, A.L., Caramelli, P., Silva, T.A., 2011. Chemokines in CSF of Alzheimer's disease patients. Arq Neuropsiquiatr 69, 455–459.

Craig-Schapiro, R., Perrin, R.J., Roe, C.M., Xiong, C., Carter, D., Cairns, N.J., Mintun, M. A., Peskind, E.R., Li, G., Galasko, D.R., Clark, C.M., Quinn, J.F., D'Angelo, G., Malone, J.P., Townsend, R.R., Morris, J.C., Fagan, A.M., Holtzman, D.M., 2010. YKL-40: a novel prognostic fluid biomarker for preclinical Alzheimer's disease. Biol. Psychiatr. 68, 903–912.

Daneman, R., Prat, A., 2015. The blood-brain barrier. Cold Spring Harbor Perspect. Biol. 7, a020412.

Delaby, C., Teunissen, C.E., Blennow, K., Alcolea, D., Arisi, I., Amar, E.B., Beaume, A., Bedel, A., Bellomo, G., Bigot-Corbel, E., Bjerke, M., Blanc-Quintin, M.C., Boada, M., Bousiges, O., Chapman, M.D., DeMarco, M.L., D'Onofrio, M., Dumurgier, J., Dufour-Rainfray, D., Engelborghs, S., Esselmann, H., Fogli, A., Gabelle, A., Galloni, E., Gondolf, C., Grandhomme, F., Grau-Rivera, O., Hart, M., Ikeuchi, T., Jeromin, A., Kasuga, K., Keshavan, A., Khalil, M., Körtvelyessy, P., Kulczynska-Przybik, A., Laplanche, J.L., Lewczuk, P., Li, Q.X., Lleó, A., Malaplate, C., Marquié, M., Masters, C.L., Mroczko, B., Nogueira, L., Orellana, A., Otto, M., Oudart, J.B., Paquet, C., Paoletti, F.P., Parnetti, L., Perret-Liaudet, A., Peoc'h, K., Poesen, K., Puig-Pijoan, A., Quadrio, I., Quillard-Muraine, M., Rucheton, B., Schraen, S., Schott, J.M., Shaw, L.M., Suárez-Calvet, M., Tsolaki, M., Tumani, H., Udeh-Momoh, C.T., Vaudran, L., Verbeek, M.M., Verde, F., Vermunt, L., Vogelgsang, J., Wiltfang, J., Zetterberg, H., Lehmann, S., 2021. Clinical Reporting Following the Quantification of Cerebrospinal Fluid Biomarkers in Alzheimer's Disease: an International Overview. Alzheimers Dement.

Dumitrescu, L., Barnes, L.L., Thambisetty, M., Beecham, G., Kunkle, B., Bush, W.S., Gifford, K.A., Chibnik, L.B., Mukherjee, S., De Jager, P.L., Kukull, W., Crane, P.K., Resnick, S.M., Keene, C.D., Montine, T.J., Schellenberg, G.D., Deming, Y., Chao, M. J., Huentelman, M., Martin, E.R., Hamilton-Nelson, K., Shaw, L.M., Trojanowski, J. Q., Peskind, E.R., Cruchaga, C., Pericak-Vance, M.A., Goate, A.M., Cox, N.J., Haines, J.L., Zetterberg, H., Blennow, K., Larson, E.B., Johnson, S.C., Albert, M., Bennett, D.A., Schneider, J.A., Jefferson, A.L., Hohman, T.J., 2019. Sex differences in the genetic predictors of Alzheimer's pathology. Brain 142, 2581–2589.

Fahrenhold, M., Rakic, S., Classey, J., Brayne, C., Ince, P.G., Nicoll, J.A.R., Boche, D., 2018. TREM2 expression in the human brain: a marker of monocyte recruitment? Brain Pathol. 28, 595–602.

Fernández-Calle, R., Konings, S.C., Frontiñán-Rubio, J., García-Revilla, J., Camprubí-Ferrer, L., Svensson, M., Martinson, I., Boza-Serrano, A., Venero, J.L., Nielsen, H.M., Gouras, G.K., Deierborg, T., 2022. APOE in the bullseye of neurodegenerative diseases: impact of the APOE genotype in Alzheimer's disease pathology and brain diseases. Mol. Neurodegener. 17, 62.

Fiala, M., Zhang, L., Gan, X., Sherry, B., Taub, D., Graves, M.C., Hama, S., Way, D., Weinand, M., Witte, M., Lorton, D., Kuo, Y.M., Roher, A.E., 1998. Amyloid-beta induces chemokine secretion and monocyte migration across a human blood–brain barrier model. Mol. Med. 4, 480–489.

Fillit, H., Ding, W.H., Buee, L., Kalman, J., Altstiel, L., Lawlor, B., Wolf-Klein, G., 1991. Elevated circulating tumor necrosis factor levels in Alzheimer's disease. Neurosci. Lett. 129, 318–320.

Forlenza, O.V., Diniz, B.S., Talib, L.L., Mendonça, V.A., Ojopi, E.B., Gattaz, W.F., Teixeira, A.L., 2009. Increased serum IL-1beta level in Alzheimer's disease and mild cognitive impairment. Dement. Geriatr. Cognit. Disord. 28, 507–512.

Frank, S., Burbach, G.J., Bonin, M., Walter, M., Streit, W., Bechmann, I., Deller, T., 2008. TREM2 is upregulated in amyloid plaque-associated microglia in aged APP23 transgenic mice. Glia 56, 1438–1447.

Fujita, M., Imaizumi, M., Zoghbi, S.S., Fujimura, Y., Farris, A.G., Suhara, T., Hong, J., Pike, V.W., Innis, R.B., 2008. Kinetic analysis in healthy humans of a novel positron emission tomography radioligand to image the peripheral benzodiazepine receptor, a potential biomarker for inflammation. Neuroimage 40, 43–52.

Galimberti, D., Fenoglio, C., Lovati, C., Venturelli, E., Guidi, I., Corrà, B., Scalabrini, D., Clerici, F., Mariani, C., Bresolin, N., Scarpini, E., 2006. Serum MCP-1 levels are increased in mild cognitive impairment and mild Alzheimer's disease. Neurobiol. Aging 27, 1763–1768.

Gao, S., Hendrie, H.C., Hall, K.S., Hui, S., 1998. The relationships between age, sex, and the incidence of dementia and Alzheimer disease: a meta-analysis. Arch. Gen. Psychiatr. 55, 809–815.

Heslegrave, A., Heywood, W., Paterson, R., Magdalinou, N., Svensson, J., Johansson, P., Öhrfelt, A., Blennow, K., Hardy, J., Schott, J., Mills, K., Zetterberg, H., 2016. Increased cerebrospinal fluid soluble TREM2 concentration in Alzheimer's disease. Mol. Neurodegener. 11, 3.

Hixson, J.E., Vernier, D.T., 1990. Restriction isotyping of human apolipoprotein E by gene amplification and cleavage with HhaI. J. Lipid Res. 31, 545–548.

Jay, T.R., Miller, C.M., Cheng, P.J., Graham, L.C., Bemiller, S., Broihier, M.L., Xu, G., Margevicius, D., Karlo, J.C., Sousa, G.L., Cotleur, A.C., Butovsky, O., Bekris, L., Staugaitis, S.M., Leverenz, J.B., Pimplikar, S.W., Landreth, G.E., Howell, G.R., Ransohoff, R.M., Lamb, B.T., 2015. TREM2 deficiency eliminates TREM2+ inflammatory macrophages and ameliorates pathology in Alzheimer's disease mouse models. J. Exp. Med. 212, 287–295.

Johnstone, M., Gearing, A.J., Miller, K.M., 1999. A central role for astrocytes in the inflammatory response to beta-amyloid; chemokines, cytokines and reactive oxygen species are produced. J. Neuroimmunol. 93, 182–193.

Karch, C.M., Goate, A.M., 2015. Alzheimer's disease risk genes and mechanisms of disease pathogenesis. Biol. Psychiatr. 77, 43–51.

Kiddle, S.J., Thambisetty, M., Simmons, A., Riddoch-Contreras, J., Hye, A., Westman, E., Pike, I., Ward, M., Johnston, C., Lupton, M.K., Lunnon, K., Soininen, H., Kloszewska, I., Tsolaki, M., Vellas, B., Mecocci, P., Lovestone, S., Newhouse, S., Dobson, R., 2012. Plasma based markers of [^{11}C] PiB-PET brain amyloid burden. PLoS One 7, e44260.

Kim, S.M., Song, J., Kim, S., Han, C., Park, M.H., Koh, Y., Jo, S.A., Kim, Y.Y., 2011. Identification of peripheral inflammatory markers between normal control and Alzheimer's disease. BMC Neurol. 11, 51.

Kiyota, T., Gendelman, H.E., Weir, R.A., Higgins, E.E., Zhang, G., Jain, M., 2013. CCL2 affects β-amyloidosis and progressive neurocognitive dysfunction in a mouse model of Alzheimer's disease. Neurobiol. Aging 34, 1060–1068.

Krstic, D., Madhusudan, A., Doehner, J., Vogel, P., Notter, T., Imhof, C., Manalastas, A., Hilfiker, M., Pfister, S., Schwerdel, C., Riether, C., Meyer, U., Knuesel, I., 2012. Systemic immune challenges trigger and drive Alzheimer-like neuropathology in mice. J. Neuroinflammation 9, 151.

Lessard, C.B., Malnik, S.L., Zhou, Y., Ladd, T.B., Cruz, P.E., Ran, Y., Mahan, T.E., Chakrabaty, P., Holtzman, D.M., Ulrich, J.D., Colonna, M., Golde, T.E., 2018. High-affinity interactions and signal transduction between Aβ oligomers and TREM2. EMBO Mol. Med. 10.

Lloret, A., Monllor, P., Esteve, D., Cervera-Ferri, A., Lloret, M.A., 2019. Obesity as a risk factor for Alzheimer's disease: implication of leptin and glutamate. Front. Neurosci. 13, 508.

Malaguarnera, L., Motta, M., Di Rosa, M., Anzaldi, M., Malaguarnera, M., 2006. Interleukin-18 and transforming growth factor-beta 1 plasma levels in Alzheimer's disease and vascular dementia. Neuropathology 26, 307–312.

McKhann, G.M., Knopman, D.S., Chertkow, H., Hyman, B.T., Jack Jr., C.R., Kawas, C.H., Klunk, W.E., Koroshetz, W.J., Manly, J.J., Mayeux, R., Mohs, R.C., Morris, J.C., Rossor, M.N., Scheltens, P., Carrillo, M.C., Thies, B., Weintraub, S., Phelps, C.H., 2011. The diagnosis of dementia due to Alzheimer's disease: recommendations from the National Institute on Aging-Alzheimer's Association workgroups on diagnostic guidelines for Alzheimer's disease. Alzheimers Dement 7, 263–269.

Meda, L., Bernasconi, S., Bonaiuto, C., Sozzani, S., Zhou, D., Otvos Jr., L., Mantovani, A., Rossi, F., Cassatella, M.A., 1996. Beta-amyloid (25-35) peptide and IFN-gamma synergistically induce the production of the chemotactic cytokine MCP-1/JE in monocytes and microglial cells. J. Immunol. 157, 1213–1218.

Nazarian, A., Yashin, A.I., Kulminski, A.M., 2019. Genome-wide analysis of genetic predisposition to Alzheimer's disease and related sex disparities. Alzheimer's Res. Ther. 11, 5.
Ohara, T., Hata, J., Tanaka, M., Honda, T., Yamakage, H., Yoshida, D., Inoue, T., Hirakawa, Y., Kusakabe, T., Shibata, M., Teraoka, T., Kitazono, T., Kanba, S., Satoh-Asahara, N., Ninomiya, T., 2019. Serum soluble triggering receptor expressed on myeloid cells 2 as a biomarker for incident dementia: the Hisayama study. Ann. Neurol. 85, 47–58.
Owen, D.R., Gunn, R.N., Rabiner, E.A., Bennacef, I., Fujita, M., Kreisl, W.C., Innis, R.B., Pike, V.W., Reynolds, R., Matthews, P.M., Parker, C.A., 2011. Mixed-affinity binding in humans with 18-kDa translocator protein ligands. J. Nucl. Med. 52, 24–32.
Papadopoulos, V., Baraldi, M., Guilarte, T.R., Knudsen, T.B., Lacapère, J.J., Lindemann, P., Norenberg, M.D., Nutt, D., Weizman, A., Zhang, M.R., Gavish, M., 2006. Translocator protein (18kDa): new nomenclature for the peripheral-type benzodiazepine receptor based on its structure and molecular function. Trends Pharmacol. Sci. 27, 402–409.
Peterson, P.K., Hu, S., Salak-Johnson, J., Molitor, T.W., Chao, C.C., 1997. Differential production of and migratory response to beta chemokines by human microglia and astrocytes. J. Infect. Dis. 175, 478–481.
Podcasy, J.L., Epperson, C.N., 2016. Considering sex and gender in Alzheimer disease and other dementias. Dialogues Clin. Neurosci. 18, 437–446.
Popp, J., Oikonomidi, A., Tautvydaitė, D., Dayon, L., Bacher, M., Migliavacca, E., Henry, H., Kirkland, R., Severin, I., Wojcik, J., Bowman, G.L., 2017. Markers of neuroinflammation associated with Alzheimer's disease pathology in older adults. Brain Behav. Immun. 62, 203–211.
Sanchez-Sanchez, J.L., Giudici, K.V., Guyonnet, S., Delrieu, J., Li, Y., Bateman, R.J., Parini, A., Vellas, B., de Souto Barreto, P., 2022. Plasma MCP-1 and changes on cognitive function in community-dwelling older adults. Alzheimer's Res. Ther. 14, 5.
Serrano-Pozo, A., Mielke, M.L., Gómez-Isla, T., Betensky, R.A., Growdon, J.H., Frosch, M. P., Hyman, B.T., 2011. Reactive glia not only associates with plaques but also parallels tangles in Alzheimer's disease. Am. J. Pathol. 179, 1373–1384.
Shi, Y., Holtzman, D.M., 2018. Interplay between innate immunity and Alzheimer disease: APOE and TREM2 in the spotlight. Nat. Rev. Immunol. 18, 759–772.
Sokolova, A., Hill, M.D., Rahimi, F., Warden, L.A., Halliday, G.M., Shepherd, C.E., 2009. Monocyte chemoattractant protein-1 plays a dominant role in the chronic inflammation observed in Alzheimer's disease. Brain Pathol. 19, 392–398.
Spatharas, P.M., Nasi, G.I., Tsiolaki, P.L., Theodoropoulou, M.K., Papandreou, N.C., Hoenger, A., Trougakos, I.P., Iconomidou, V.A., 2022. Clusterin in Alzheimer's disease: an amyloidogenic inhibitor of amyloid formation? Biochim. Biophys. Acta, Mol. Basis Dis. 1868, 166384.
Tzourio-Mazoyer, N., Landeau, B., Papathanassiou, D., Crivello, F., Etard, O., Delcroix, N., Mazoyer, B., Joliot, M., 2002. Automated anatomical labeling of activations in SPM using a macroscopic anatomical parcellation of the MNI MRI single-subject brain. Neuroimage 15, 273–289.
Ulrich, J.D., Finn, M.B., Wang, Y., Shen, A., Mahan, T.E., Jiang, H., Stewart, F.R., Piccio, L., Colonna, M., Holtzman, D.M., 2014. Altered microglial response to Aβ plaques in APPPS1-21 mice heterozygous for TREM2. Mol. Neurodegener. 9, 20.
Viña, J., Lloret, A., 2010. Why women have more Alzheimer's disease than men: gender and mitochondrial toxicity of amyloid-beta peptide. J Alzheimers Dis 20 (Suppl. 2), S527–S533.
Wong, D., Dorovini-Zis, K., Vincent, S.R., 2004. Cytokines, nitric oxide, and cGMP modulate the permeability of an in vitro model of the human blood-brain barrier. Exp. Neurol. 190, 446–455.
Wu, Y.Y., Hsu, J.L., Wang, H.C., Wu, S.J., Hong, C.J., Cheng, I.H., 2015. Alterations of the neuroinflammatory markers IL-6 and TRAIL in Alzheimer's disease. Dement Geriatr Cogn Dis Extra 5, 424–434.
Wunderlich, P., Glebov, K., Kemmerling, N., Tien, N.T., Neumann, H., Walter, J., 2013. Sequential proteolytic processing of the triggering receptor expressed on myeloid cells-2 (TREM2) protein by ectodomain shedding and γ-secretase-dependent intramembranous cleavage. J. Biol. Chem. 288, 33027–33036.
Xie, Z., Harris-White, M.E., Wals, P.A., Frautschy, S.A., Finch, C.E., Morgan, T.E., 2005. Apolipoprotein J (clusterin) activates rodent microglia in vivo and in vitro. J. Neurochem. 93, 1038–1046.
Yasuno, F., Kimura, Y., Ogata, A., Ikenuma, H., Abe, J., Minami, H., Nihashi, T., Yokoi, K., Hattori, S., Shimoda, N., Ichise, M., Sakurai, T., Ito, K., Kato, T., 2022. Kinetic modeling and non-invasive approach for translocator protein quantification with (11)C-DPA-713. Nucl. Med. Biol. 108–109, 76–84.
Yasuno, F., Kosaka, J., Ota, M., Higuchi, M., Ito, H., Fujimura, Y., Nozaki, S., Takahashi, S., Mizukami, K., Asada, T., Suhara, T., 2012. Increased binding of peripheral benzodiazepine receptor in mild cognitive impairment-dementia converters measured by positron emission tomography with [^{11}C]DAA1106. Psychiatr. Res. 203, 67–74.
Yasuno, F., Ota, M., Kosaka, J., Ito, H., Higuchi, M., Doronbekov, T.K., Nozaki, S., Fujimura, Y., Koeda, M., Asada, T., Suhara, T., 2008. Increased binding of peripheral benzodiazepine receptor in Alzheimer's disease measured by positron emission tomography with [^{11}C]DAA1106. Biol. Psychiatr. 64, 835–841.
Yusufov, M., Weyandt, L.L., Piryatinsky, I., 2017. Alzheimer's disease and diet: a systematic review. Int. J. Neurosci. 127, 161–175.
Zhang, B., Gaiteri, C., Bodea, L.G., Wang, Z., McElwee, J., Podtelezhnikov, A.A., Zhang, C., Xie, T., Tran, L., Dobrin, R., Fluder, E., Clurman, B., Melquist, S., Narayanan, M., Suver, C., Shah, H., Mahajan, M., Gillis, T., Mysore, J., MacDonald, M.E., Lamb, J.R., Bennett, D.A., Molony, C., Stone, D.J., Gudnason, V., Myers, A.J., Schadt, E.E., Neumann, H., Zhu, J., Emilsson, V., 2013. Integrated systems approach identifies genetic nodes and networks in late-onset Alzheimer's disease. Cell 153, 707–720.
Zhao, Y., Wu, X., Li, X., Jiang, L.L., Gui, X., Liu, Y., Sun, Y., Zhu, B., Piña-Crespo, J.C., Zhang, M., Zhang, N., Chen, X., Bu, G., An, Z., Huang, T.Y., Xu, H., 2018. TREM2 is a receptor for β-amyloid that mediates microglial function. Neuron 97, 1023–1031 e1027.
Zhong, L., Xu, Y., Zhuo, R., Wang, T., Wang, K., Huang, R., Wang, D., Gao, Y., Zhu, Y., Sheng, X., Chen, K., Wang, N., Zhu, L., Can, D., Marten, Y., Shinohara, M., Liu, C.C., Du, D., Sun, H., Wen, L., Xu, H., Bu, G., Chen, X.F., 2019. Soluble TREM2 ameliorates pathological phenotypes by modulating microglial functions in an Alzheimer's disease model. Nat. Commun. 10, 1365.
Zujovic, V., Benavides, J., Vigé, X., Carter, C., Taupin, V., 2000. Fractalkine modulates TNF-alpha secretion and neurotoxicity induced by microglial activation. Glia 29, 305–315.